Supporting Information: Plasmonic Nanostructure Design for Efficient Light Coupling into Solar Cells

Vivian E. Ferry, Luke A. Sweatlock, Domenico Pacifici, Harry A. Atwater
Thomas J. Watson Laboratories of Applied Physics
California Institute of Technology
Pasadena, CA 91125

Our analysis is based on the calculation of incoupling cross sections for a variety of nanostructured scattering objects which couple incident light to guided modes.[1–3] The cross section corresponds to the amount of incident light that is captured by the object, which may be much larger than its physical size. The goal of this section is to describe our method for assessing the incoupling ability of these structures, and for tracking the dissipation of power that enters the device. Incident light is scattered from the groove and may be coupled into propagating modes, which are subsequently absorbed in either the semiconductor or the metal. Some of the optical power backscattered at angles near normal is lost by transmission through the top surface. Additionally, there are fundamental thin film processes such as reflection, transmission, and absorption, that occur in the device without necessarily interacting with the scatterer.

As an example, consider a 200 nm Si slab on 300 nm of Ag, with a 100 nm wide by 50 nm deep groove cut into the Ag. The structure is illuminated at normal incidence by a continuous wave source ($\lambda = 1000$ nm) polarized transverse magnetic (TM), i.e. with the

H field directed along the long axis of the groove. The source plane is located 2 μm above the Si/Ag interface. In Figure 1a, the interface is located at x = -1 μm, and the beam is launched at x = 1 μm. The two-dimensional simulation volume is 10 μm long, with the scattering object at the center, and 4 μm tall. A uniform mesh size of 5 nm is used for the entire volume, and perfectly matched layers (PML) are used at the boundaries. Silver and aluminum are modeled as Lorentz-Drude dielectric functions using the method of Rakic et al.,[4] and the optical constants for Si and GaAs from 400 - 1100 nm are taken from Palik.[5]

A full-field simulation of this device generates a complicated field pattern from the interference of the incident beam ($\mathbf{H}_{inc}$) with the fields reflected from the smooth metal surface ($\mathbf{H}_{ref}$) and those scattered by the groove ($\mathbf{H}_{scat}$). Since we are working with complex-valued time harmonic fields, it is straightforward to isolate the scattered fields by employing a linear subtraction method. We first perform a full-field simulation where the interference pattern is generated by the sum of these three component fields $\mathbf{H}_{total} = \mathbf{H}_{inc} + \mathbf{H}_{ref} + \mathbf{H}_{scat}$. A second control simulation is then performed with a smooth metal surface without any groove. Here $\mathbf{H}_{control} = \mathbf{H}_{inc} + \mathbf{H}_{ref}$. The other parameters are identical, so we determine the scattered fields by subtraction, $\mathbf{H}_{scat} = \mathbf{H}_{total} - \mathbf{H}_{control}$. Figure 1 shows the isolated scattered fields for two different nanostructures in the Ag film, a groove and a ridge. The remaining interference pattern is due to the presence of multiple modes in the waveguide. The difference in these two scattering responses motivates the development of our FMSA technique to decompose the individual modes.

The post-processing method takes a map of each of the three electromagnetic field components $(E_x(x,z), H_y(x,z), E_z(x,z))$ as input, which are then transformed to wavevector space $(e_x(x,k), h_y(x,k), e_z(x,k))$ using a one dimensional fast Fourier transform (FFT). The x-position remains unchanged. To visualize the energy content of the modes, we calculate a power spectrum for each field: $|h_y(x,k)|^2 = h_y(x,k)h_y^*(x,k)$. Figure 1a shows

these Fourier-space power spectra. The horizontal axis is the spatial frequency, and the vertical axis records the position in the waveguide. We see two bright spots within the device, centered at 2 μm^{-1} and 4.2 μm^{-1}; each of these peaks represents a mode. Within the core of the waveguide, the mode at 2 μm^{-1} has one bright spot vertically, and a second one at the metal-semiconductor interface. This spatial mode profile is somewhat similar to that of a conventional dielectric waveguide mode, and by analogy we designate it as a photonic mode. The peak at 4.2 μm^{-1} has a higher spatial frequency and is localized at the interface, indicating that it is the SPP mode.

Cross sections of this data set along either axis reveal other characteristics of the system. Figure 1b plots the Fourier power spectrum $|h_y|^2$ as a function of spatial frequency, at three different x-positions in the device. At the top Si/air interface (x = -0.8 μm) we observe only the photonic mode, in the middle of the Si layer we see the SPP mode begin to come in, and at the Si/Ag interface (x = -1 μm), we observe a superposition of both modes. Figure 1c represents the other cross-section of Figure 1a, the spatial mode profile, or Fourier power spectrum as a function of position. The cuts are taken at the peak frequencies observed in Figure 1b, allowing us to visualize the power localization within the waveguide. The SPP peak at 4.2 μm^{-1} is shown in red; it is confined to the Si/Ag interface, and the power falls off exponentially on each side. The photonic mode at 2 μm^{-1} is plotted in blue, and we confirm that it is the lowest order mode.

Since the modes are distinguishable by their wavevector k in Fourier space, we can perform modal analysis that is not possible in Cartesian (x, z) space. Our method uses a Fourier-space notch filter to isolate each mode. The notch filter is perfectly rectangular, and of the form

$$f(k) = \begin{cases} 0 & \text{if } |k| < k_{low} \\ 1 & \text{if } k_{low} < |k| < k_{high} \\ 0 & \text{if } |k| < k_{low} \end{cases}$$

These filtered sets are then transformed back to real space, producing an image of each individual mode. Figure 1d and e show the H_y component of the filtered fields after transforming back to Cartesian coordinates; the top image is the photonic mode, and the bottom the SPP mode.

We are most interested in connecting these data sets to the energy content of each mode and the incoupling efficiency of the scattering object. The energy flow in the structure is calculated using the time-harmonic form of Poynting's theorem

$$< \mathbf{S} >= \frac{1}{2}\Re(\mathbf{E}_{scat} \times \mathbf{H}^*_{scat})$$

where $\mathbf{E}_{scat}$ is the scattered electric field (E_x and E_z components) and $\mathbf{H}^*_{scat}$ is the complex conjugate of the magnetic field (H_y component). This calculation is done for each of the filtered data sets.

We then draw an enclosing pillbox around the structure at a height h that encompasses the majority of the modal energy which extends outside the waveguide, and a variable length l. The line integral through the Poynting vector plot on each side of the box gives the time average power flow in that direction: the top measures the backscattered component, the bottom measures any transmission which occurs through the metal film, and the components flowing to the sides measure the power in the guided modes. A schematic of the box drawn around the film is shown in Figure 2.

$$U_{backscatter} = \int_{5-\frac{l}{2}}^{5+\frac{l}{2}} S_x(x = h, z)dz$$

$$U_{guided} = \int_{-1.3}^{h} S_z(x, z = 5 + \frac{l}{2})dx$$

The box is symmetric around the groove, with the center located at $z = 5$ μm. The Ag/air interface is at x = -1.3 μm, and none of the modes extend substantially outside the back surface of the metal. The extent of the mode outside the semiconductor varies by wavelength, and so the pillbox height h may vary across the spectrum. At a given frequency and constant h, we step through a number of box lengths, thus monitoring the power flow as a function of distance from the groove. The entire data set is normalized by the incident power that hit the top of the device in a 1 μm wide region, from 4.5 μm $< z <$5.5 μm.

$$U_{incident} = \int_{4.5}^{5.5} S_{x,incident}(x = -0.8, z)dz$$

where $S_{x,incident}$ is from a separate control simulation of the propagating incident light in the absence of a device.

The guided modes are lossy, so we calculate the attenuation during propagation by observing the power flow at multiple lengths l. The attenuation is expected to be of exponential form, and so we can observe the power at points any distance from the groove and fit to extract the value at $\frac{l}{2} = 0$. Figure 3 shows an example of the power decay as a function of groove distance for $\lambda_{excitation}$ = 1000 nm. Here we calculate the normalized power flow slices for 0.625 μm $< \frac{l}{2} <$4.5 μm. The same calculation is done on each side of the groove, to account for modes launched in both directions on excitation. After normalization, we call this extracted value the incoupling cross section σ_{inc}. This cross section describes the physical area of light harvested by the groove, which may be much larger than it's physical dimensions. For a 2D simulation, the cross section has units of length rather than area as in a 3D simulation, and so it is comparable to an effective width

of the structure.

References

[1] A.-L. Baudrion, F. de Leon-Perez, O. Mahboub, A. Hohenhau, et al., *Opt. Express* **16**, 3420 (2008).

[2] H.W. Kihm, K.G. Lee, D.S. Kim, J.H. Kang, Q-H. Park, *Appl. Phys. Lett.* **92**, 051115 (2008).

[3] G. Leveque, O.J.F. Martin, J. Weiner, *Phys. Rev. B* **76**, 155418 (2007).

[4] A.D. Rakic, A.B. Djurisic, J.M. Elazar, M.L. Majewski, *Appl. Opt.* **37**, 5271 (1998).

[5] E. Palik and G. Ghosh, *Handbook of Optical Constants of Solids II*, Academic Press, New York, 1991.

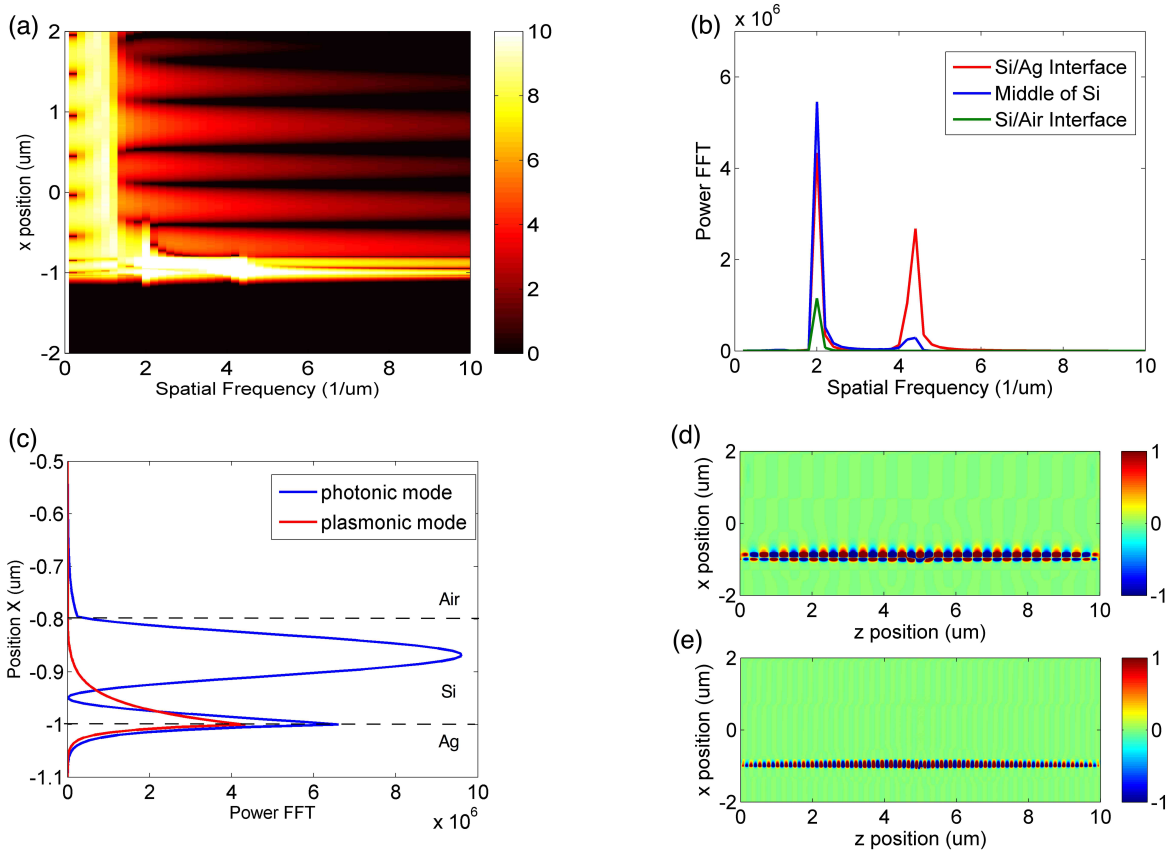

Figure 1: Method for isolating waveguide modes, shown at $\lambda = 1000$ nm for 200 nm of Si on 300 nm of Ag. Panel a shows the one dimensional Fourier transform of figure 1b, where the z axis is transformed and the x axis is unchanged. Panel b is the horizontal cross-cut of panel a, showing the frequencies of the modes present at different heights in the waveguide. Panel c is the vertical cross cut of panel a, taken at the frequencies found in panel b, and shows the spatial distribution of the power in each mode. The mode that exponentially decays away from the Si/Ag interface (red) is identified as the SPP mode, and the mode shown in blue is a second waveguide mode. Panels d and e show the H_y field of each mode after filtering in Fourier space and transforming back to real space. Panel d corresponds to the photonic mode in panel c, and panel e is the SPP mode of panel c.

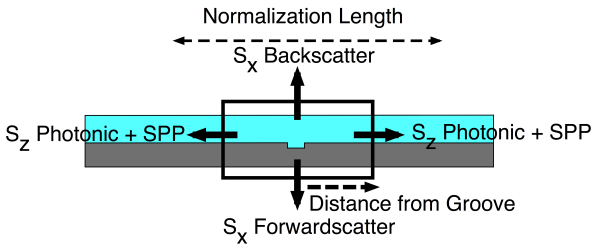

Figure 2: Schematic showing the pillbox surrounding the groove. Line integrals are calculated on the poynting vector on each side of the box for the guided modes, backscattering, and forward scattering.

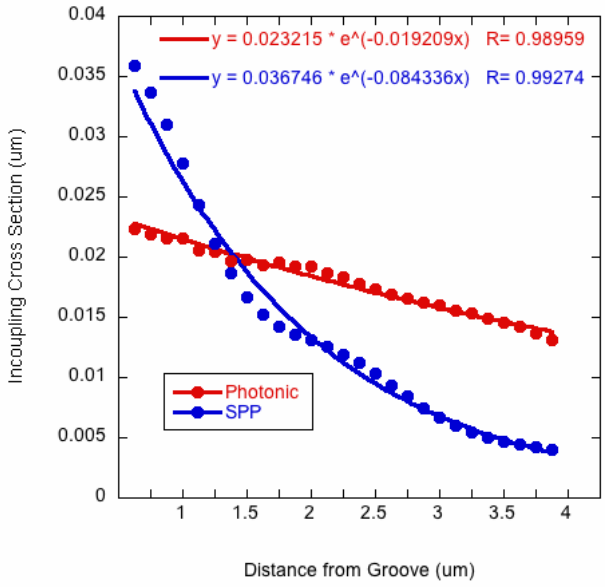

Figure 3: For each mode, the line integrals of Sz through the width of the waveguide are plotted at increasing distance from the groove centerpoint. This measures the power decay in each mode, which we fit to an exponential curve to back out the value at the origin (groove mouth). All of the numbers are normalized by the power incident on the top of the Si over a 1 μm area surrounding the groove to give an effective size. This data set is for 1000 nm incident light, and a 100 nm x 50 nm groove in 200 nm Si, and shows only the modes moving in the +z direction.